Particle Wetting Distribution in Trickle-Bed Reactors

Arie Jan van Houwelingen, Carl Sandrock, and Willie Nicol
University of Pretoria, Pretoria 0002, South Africa

DOI 10.1002/aic.10961
Published online August 2, 2006 in Wiley InterScience (www.interscience.wiley.com).

A novel technique is used to obtain the distribution of particle wetting in trickle-bed reactors for different flow and prewetting conditions. Two prewetting methods were investigated: (1) Levec prewetting, in which the packed catalyst bed is completely flooded and then left to drain before steady state trickle-flow is commenced; (2) Kan prewetting, in which the bed is prewetted by pulsing with the liquid before flow, after which the liquid flow is gradually set back to the required rate. It is shown that the method of prewetting has a major influence on average wetting efficiency and wetting distributions: Average wetting efficiencies differ with as much as 20% between the prewetting modes, and Levec prewetting leads to a considerable fraction of the bed that is not used (up to 7% at the investigated flow conditions), whereas the entire catalyst is used in Kan prewetted beds. It is shown that the particle wetting distributions can influence the modeling of Levec prewetted beds for liquid- and gas-limited conditions. © 2006 American Institute of Chemical Engineers *AIChE J,* 52: 3532–3542, 2006
Keywords: trickle-bed reactors, wetting efficiency, trickle-flow, solid-liquid contacting efficiency

Introduction

Trickle-bed reactors (TBRs) are catalytic three-phase reactors where gas and liquid reagents flow concurrently down a packed catalyst bed, and find their main applications in oil refining and petrochemical and biochemical processes. To model these reactors, liquid flow over the catalyst bed is traditionally described in terms of bed-averaged hydrodynamic parameters such as the percentage of liquid in the reactor (liquid holdup), two-phase pressure drop, and the fraction of external catalyst area that is exposed to the flowing liquid (wetting efficiency). The latter is believed to directly influence the efficiency of a trickle-bed reactor compared to that of an ideal plug flow reactor because of its influence on the external and internal mass transfer rates[1]:

$$\frac{dF_A}{dW} = -r_A \eta_{TB} \tag{1}$$

where the trickle-bed efficiency (η_{TB}) is a function of the wetting efficiency (f_{avg}).

Numerous models exist that relate these two quantities, most of which are based on particle-scale phenomena.[1-4] According to these models, the relationship between a particle's efficiency and the fraction of its area that is exposed to the liquid is nonlinear. This suggests that not only the average wetting efficiency, but also the distribution of particle wetting (that is, how many particles are wetted to what extent) can be of importance.

A typical example of how the particle wetting distribution (PWD)—and not only the average wetting efficiency—can be of importance was illustrated by Beaudry et al.[4] for *gas-limited reactions*. As a rule, the efficiency of a particle will increase with decreasing fractional wetting. However, when the wetting efficiency becomes too low, depletion of the nonvolatile reagent in the particle will lead to decreasing performance with

Correspondence concerning this article should be addressed to W. Nicol at willie.nicol@up.ac.za.

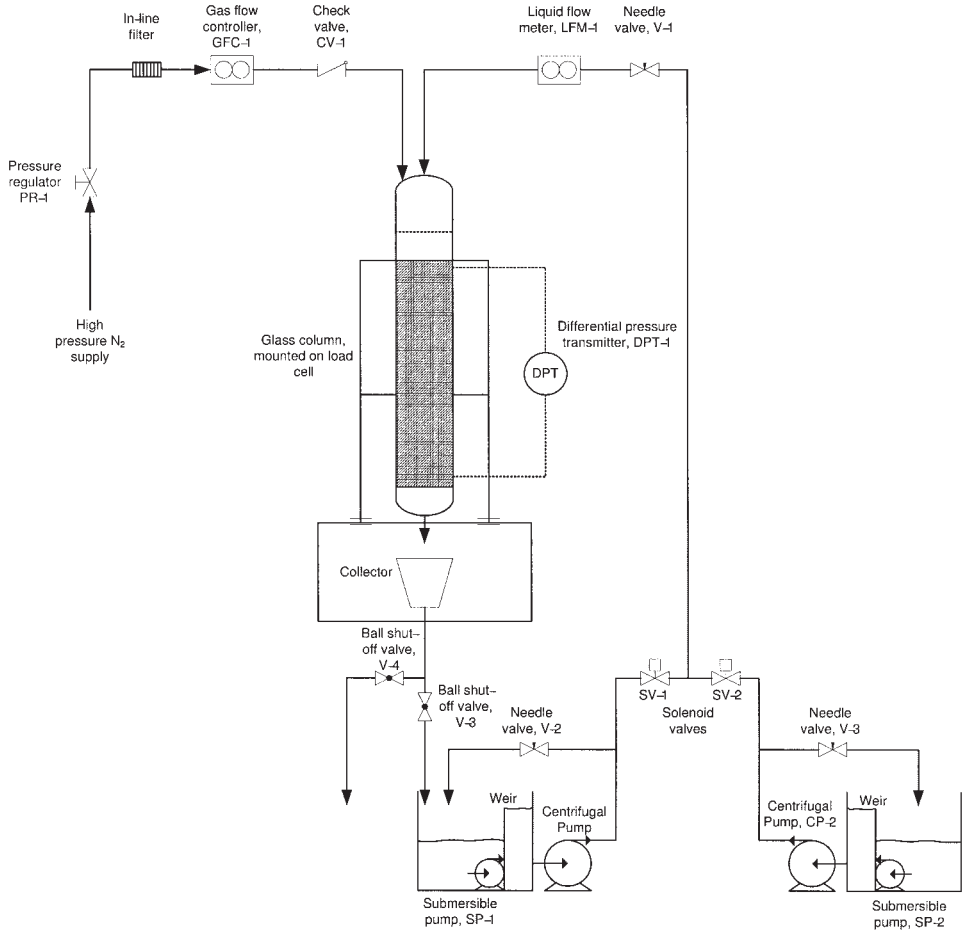

Figure 1. Flow diagram of the experimental setup.

decreasing fractional wetting. A low average wetting may therefore be either beneficial or detrimental for reactor performance, depending on whether the fractional wetting of all particles is close to the average wetting or whether the low average wetting is caused by very poorly wetted particles that exhibit liquid limitations. To account for this possibility, they assumed that the PWD in trickle-bed reactors consists of completely dry, half-wetted, and completely wetted particles, the fraction of each being related to the average wetting efficiency in the following fashion:

$$P(f)|_{f=0}| = (1 - f_{avg})^2$$
$$P(f)|_{f=0.5}| = 2(1 - f_{avg}) f_{avg}$$
$$P(f)|_{f=1}| = f_{avg}^2 \quad (2)$$

No evidence exists that this assumption is accurate.

Ever since Kan and Greenfield[5] found flow hysteresis in trickle-bed reactors, multiple hydrodynamic states in trickle flow have been studied by numerous authors.[6-8] Several studies show that the hydrodynamic state of trickle flow may be manipulated by means of the procedure according to which a bed is prewetted before flow.[8-10] Flow hysteresis and multiple hydrodynamic states are mostly quantified by pressure drop and holdup measurements.[5,6,10-12] Differences in liquid flow morphology or shape are normally used to explain the existence of multiple hydrodynamic states[6,10]; and computer-assisted tomography visualizations support this belief.[7,9] Popular descriptions of trickle-flow morphologies suggest that the distribution and nature of wetting efficiency may be functions of flow morphology, although no attempt has been made to quantify this.[6,9,13]

In this article a novel technique is used to obtain PWDs for an atmospheric N_2–water trickle-flow system at different operating conditions. In addition different prewetting procedures are used to obtain PWDs for multiple hydrodynamic states. Finally, the effect of the PWDs of the different hydrodynamic states on trickle-bed reactor modeling and performance is briefly discussed.

Experimental

Setup

Figure 1 shows the process flow diagram of the experimental setup. This setup consists of a packed column with distributor, a low pressure N_2 feed system, and two separate liquid feed systems, one for clear water feed and one for water doped with a colorant.

The column consists of a 1.0-m long, 63-mm inner diameter

Table 1. Experimental Flow Conditions

L (kg m^{-2} s^{-1})	G (kg m^{-2} s^{-1})	Prewetting Procedure
1.60	0.023	Kan
1.60	0.152	Kan
1.60	0.152	Levec
5.35	0.023	Kan
5.35	0.152	Kan
5.35	0.152	Levec

tube that is packed with 2.5-mm diameter γ-alumina spheres. The column is made from glass so that the flow patterns can be observed during trickle flow. Liquid is introduced in the bed through a distributor cap, with a liquid drip point density of 16,000 points/m^2, which is well above the 5000 points/m^2 recommended for a uniform liquid inlet distribution.[14] The gas enters the bed through three equilaterally spaced 1/4-in. tubes, 10 mm from the center point of the column.

The clear water feed is used to prewet each bed and for attainment of steady-state trickle flow. Steady flow is identified by means of pressure drop and holdup measurements and by visual observation through the glass column wall. After steady flow is obtained, the feed is switched to the tank that contains a 0.2 g/L solution of the colorant Chrome Azurol S. Liquid recycle lines with needle valves are installed around both feed tanks, which can be used to minimize disturbances during feed switchover.

Areas on each particle in contact with the Chrome Azurol S solution exhibit a deep red color. This colorant was previously used successfully for the determination of wetting efficiency and has the primary advantage that it adsorbs irreversibly onto the external γ-alumina surface without diffusing through the particles, thereby coloring only the surfaces that were in contact with the liquid.[15] The color intensity of the contacted surfaces become independent of contacting time after about 20 min, and colorant flow was maintained at steady state for about 40 min to avoid an axial color intensity profile through the bed because colorant is initially stripped from its solution in the top of the bed. Flow is then switched back to clear water at the same flow conditions until the colorant is washed out, after which it is drained and allowed to dry.

Liquid holdup is measured by means of a load cell (±4 g accuracy) on which the column is mounted, whereas the liquid flow is adjusted by means of a needle valve and monitored by means of an electromagnetic flow meter with an accuracy of ±0.5% of the flow rate. The gas flow is controlled and monitored by means of a Brooks Smart mass flow controller (±0.7% of flow rate). Data from these instruments were logged, so that the stability of flow can be verified during and after an experiment.

Inherent to colorimetric methods lies the assumption that trickle flow is stable during steady state: flow fluctuations will lead to an overestimation of wetting efficiency. This assumption is supported by data from Van der Merwe and Nicol[10] and the observations of Sederman and Gladden.[9] It is also likely that flow instabilities will show in color intensity variations of the particle surfaces that were in contact with the colorant. No significant variations were observed.

Prewetting procedure and flow conditions

The work of Sederman and Gladden[9] and Van der Merwe and Nicol[10] suggests that the morphology of liquid flow in a trickle-bed reactor can be manipulated by means of the manner in which the bed is prewetted. The following procedures were adopted:

- *Levec prewetting*. Before liquid irrigation, the bed is kept completely submersed in water for at least 3 h to ensure complete internal saturation[16] and complete external wetting of all particles. The bed is then drained under experimental gas flow conditions until only the residual liquid holdup remains, after which liquid irrigation at the required rate is introduced. The rate of evaporation attributed to gas flow was found to be insignificant compared to the rate of draining. Note that this Levec prewetting procedure does deviate from the procedure stated by Wang et al.,[12] who drained the bed without gas flow and prewetted the packing by pulsing with the liquid instead of flooding. In both cases, however, only the residual holdup remains before commencement of flow.
- *Kan prewetting*. After the packing is internally saturated, the bed is drained and gas flow is set to the required rate. Liquid flow is increased until the pulsing regime is encountered and is then gradually set back to the required rate.

Experimental flow conditions are shown in Table 1.

Particle sampling and analysis

After the bed is dry, the particles in the bed are unloaded and mixed, so that the sample particles are representative of the particles in the bed. These sample particles are captured in a sampling grid, a plate in which a 17 × 17 grid of 2.7-mm holes are drilled. Particles in the grid are retained by two clear PVC plates that are fastened on both sides of the grid and are then photographed in a light box, as shown in Figure 2, to obtain consistent images. The grid is photographed from two sides, so

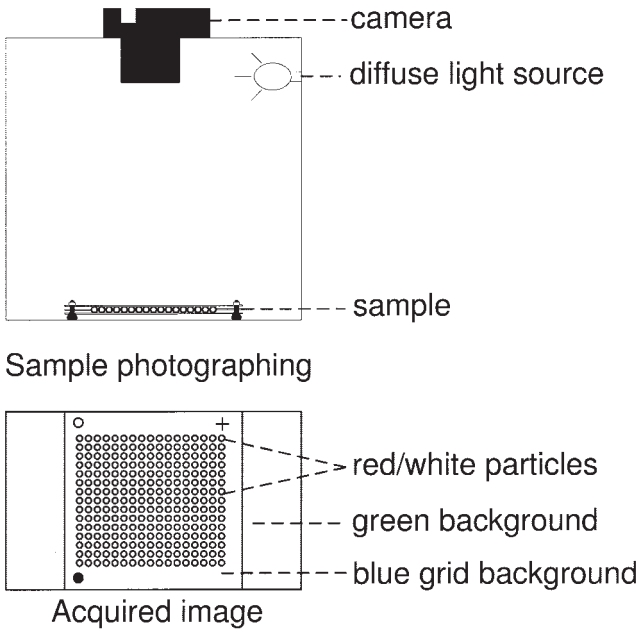

Figure 2. Particle sampling.

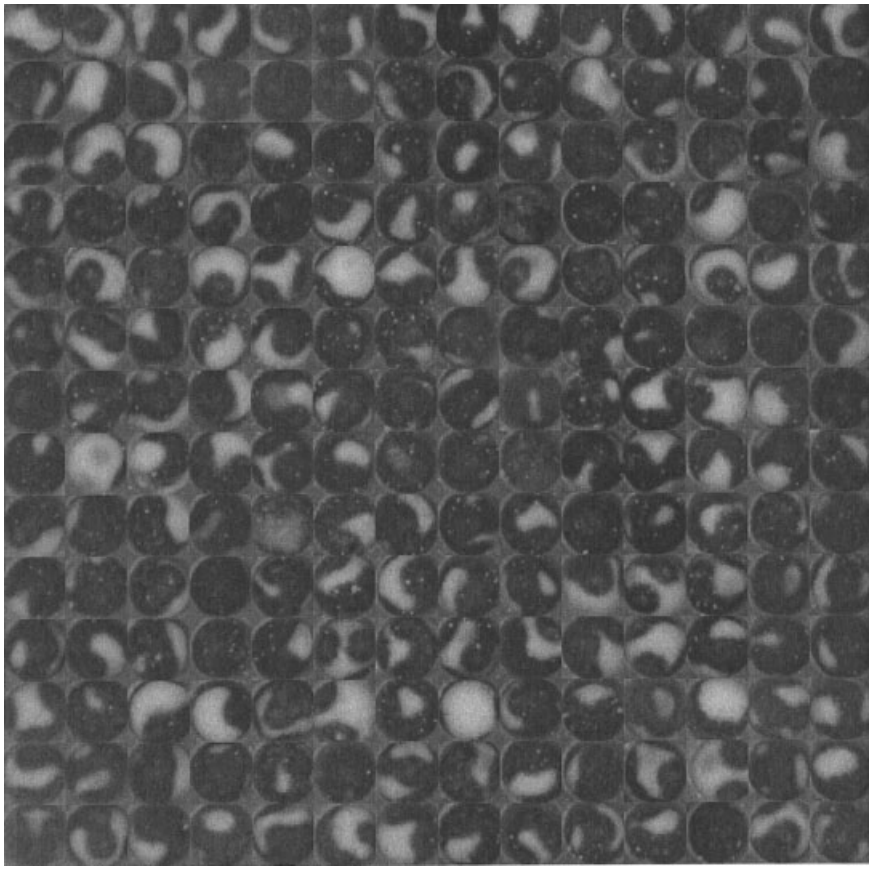

Figure 3. An example of analyzed half-particle images.

that two sides of each specific particle are known and the largest possible area can be evaluated. Fifteen samples of 17 × 17 particles were used to characterize each bed.

By use of the Image Processing toolbox of Matlab® (The MathWorks, Natick, MA), half-particles are identified and extracted from the image and the wetted fraction of each half-particle is calculated. To simplify the extraction process, the grid color was chosen as blue, resulting in a good contrast between the grid and the particles when a red filter is applied to the images. Background color was chosen as green, for easy realignment of the image if it is skewed. Each half-particle is extracted as a separate image and each pixel on these images is classified as wetted or nonwetted based on its color. Because each image is a two-dimensional (2-D) projection of a three-dimensional (3-D) hemisphere, the contribution of each pixel was weighted according to the 3-D area that it represents. Half-particles are then matched to give the wetting efficiency of each particle. Reference points for the matching of half-particles are supplied by markings on the grid. An example of the extracted half-particle images is shown in Figure 3.

Data Accuracy

Particle measurements

The pixel analysis is straightforward, except for the pixels on the boundary of the 2-D projection of each half-particle. At the particle boundaries, pixels can easily be incorrectly classified. This was primarily a result of color smudge (which is attributed to the format of the digital images), loose pick-up of the particles (a small ring of pixels surrounding a particle image is classified as being part of it by the particle extraction program), and shadows on the image. This boundary effect is illustrated in Figure 4. Being a 2-D projection of a hemisphere, the boundary pixels represent a very large fraction of the true spherical area and incorrect classification of their wetting leads to substantial errors in the estimation of the wetting of a particle. Any boundary pixel that can be incorrectly classified therefore needs to be discarded. As a result only a part of the area of the particles can be evaluated, and instead of the full hemisphere each image represents, only a spherical cap with base radius $r<R$ can be evaluated for each image.

Because the area fraction that is taken into account is such a strong function of r/R, it is important to discard as few as possible rings of boundary pixels, but enough to avoid the large errors that are caused by the boundary effect. To find this optimum "operating point," the apparent wetted fraction of a completely wetted, completely dry, and partially wetted particle was calculated as a function of r/R. Results are shown in Figure 5. It can be seen from the figure that all pixels further away than $r/R = 0.91$ from the center point had to be discarded because of the boundary effect (the outer three rings of pixels in the 70 × 70 pixels image exhibit boundary errors). This means that only 60% of the total area of a particle can be taken into account.

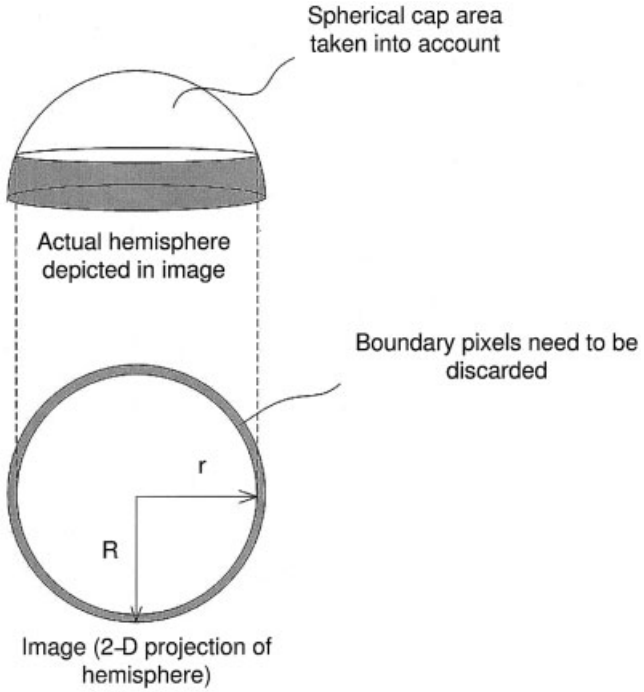

Figure 4. Boundary effect: blurriness around edges of particles has as a result that some of the outer pixels of the 2-D image must be discarded.

This translates into a large spherical area that cannot be taken into account.

If only 60% of each particle's area can be evaluated, it is necessary to evaluate whether the particle wetting distributions that are obtained are representative of the true particle wetting distributions. This will be the case only if the PWDs are not strongly dependent on the amount of area evaluated. PWDs in this work are presented as histograms with bin size 0.05. That is, the fractions of particles with wetting efficiencies within a range of size 0.05 are reported for each PWD.

Figure 6 shows the dependency of some PWD histogram bins on the fractional area that was taken into account for the evaluation of each particle. Fifteen samples taken from a Kan prewetted bed with $L = 5.35$ kg m^{-2} s^{-1} and $G = 0.023$ kg m^{-2} s^{-1} were used to construct this figure. (The histogram for these experimental operating conditions is shown later in Figure 11.) Three bins are shown: (1) one bin that is near the peak of the distribution ($0.75 < f_n < 0.8$), that is, a large amount of the particles have an evaluated fractional wetting within this bin range; (2) one bin to the right of this peak ($0.95 < f_n < 1.0$); and (3) one bin to the left of this peak ($0.55 < f_n < 0.6$).

As the evaluated area fraction is increased, the evaluated fraction of particles in the bins near the peak of the PWD increases, whereas the fraction of particles in the bins removed from the PWD peak is decreased. That is, the distribution becomes sharper (higher peak, less variance). It can therefore be concluded that the obtained PWDs are flatter (lower peak, more variance) than the true PWDs. This error can be estimated by extrapolating the curve of the bin at the peak of the PWD ($0.75 < f_n < 0.8$); the true distribution will have a peak that exceeds the presented PWDs with about 0.025. Note that some of the PWDs presented in the results section have two peaks, and that both peaks become sharper as more area is taken into account. The estimated error reported above is similar for all obtained PWDs.

The preceding error estimation makes use of considerable extrapolation and thus verification is necessary. The extrapolation of the "completely wetted" bin ($0.95 < f_n < 1.0$) was verified, by filling the sampling grid with well-wetted and completely wetted particles. The well-wetted particles were visually verified to have a fractional wetting > 0.5. Before photographing the grid, the positions of the completely wetted particles are noted, and the extrapolation validity can be verified with respect to the amount of particles that were correctly classified. Results are shown in Figure 7. With 60% of the area taken into account, >95% of all particles were classified correctly.

Population size

In this investigation, a packed bed contained between 300,000 and 400,000 particles, whereas only about 250 particles could be photographed and analyzed at a time. It therefore has to be ensured that enough samples were taken from the bed to obtain representative PWDs. Figure 8 shows the average wetting efficiencies for 15 different samples from the same bed. It is clear that even only one sample is quite representative of the bed in terms of the average wetting efficiency: all values are within 4% of the mean.

For the shape of the distribution, the standard deviation (SD) is of importance. For 15 bed samples, the SD values varied

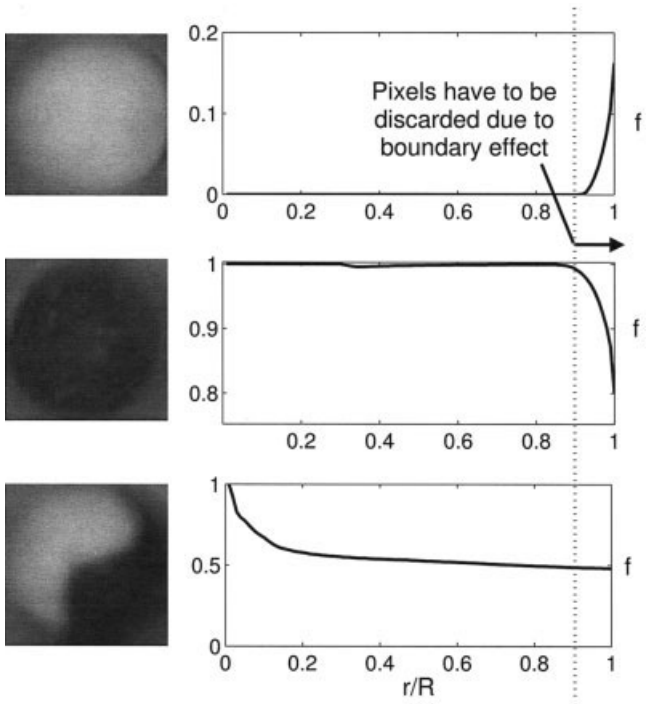

Figure 5. Estimation of the maximum distance *r* from the center point for which pixels can be taken into account.

Sudden errors in the evaluated fractional wetting of the completely wetted and completely dry particles indicate the boundary effect.

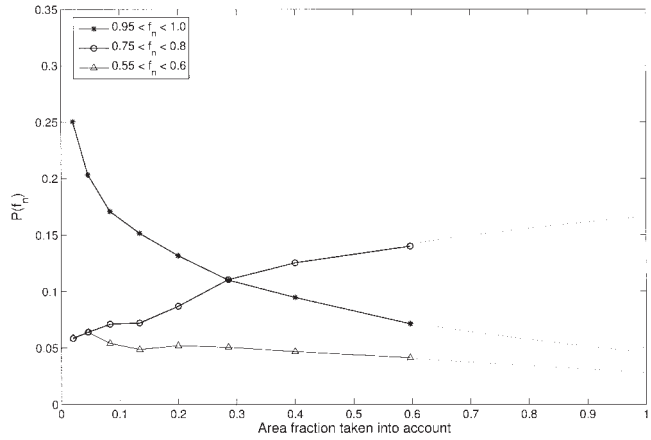

Figure 6. Dependency of histogram bins of the particle wetting distribution on the area fraction that is taken into account.

Visual extrapolation of the functions are provided in a dotted line.

with a maximum of 15% from the mean, and one sample is clearly not representative of the bed in terms of the SD of the particle wetting efficiency distribution. For the PWDs to be statistically representative, the value of the total population SD should converge within the 15 samples that were taken from the bed. A sample SD as a function of sample size is shown in Figure 9. The SD does not change significantly after the population size has reached 2000 particles, and it is clear that 15 samples (about 4000 particles) are sufficient to determine the SD of the distribution. Data from other experiments lead to the same conclusion.

Results

Operational measurements

Liquid holdup and pressure drop measurements for all flow conditions are shown in Table 2. Average wetting efficiencies are compared to existing data and correlations[17-21] in Figure 10.

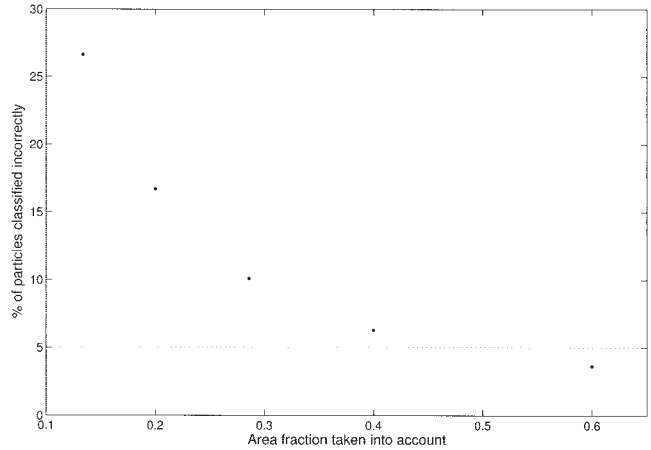

Figure 7. Error in classification between completely wetted and well-wetted particles as a function of the fractional area taken into account.

Population size was 1200 particles.

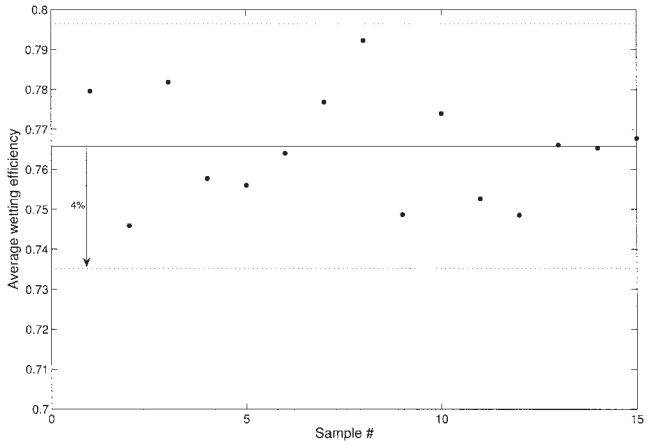

Figure 8. Average wetting efficiencies for different samples from the same bed.

Particle wetting distributions

Kan Prewetted Beds. PWDs for the Kan prewetted beds at two different experimental liquid flow rates and at G values of 0.023 and 0.152 kg m^{-2} s^{-1} are depicted as histograms with bin size 0.05 in Figures 11 and 12. In the figures, the quantity $P(f_n)$ is the fraction of particles with a fractional wetting f, where $f_n - 0.025 < f < f_n + 0.025$. The light gray color is a result of overlap of the two distributions. Smooth curves are drawn through the distributions for the purpose of better visualization. Figures 13a and 13b show the same PWDs plotted together for constant liquid flow rate and different gas flow rates, to illustrate the effect of increasing gas flow rate.

Levec prewetted beds

PWDs for the Levec prewetted beds are shown in Figure 14. Figures 15a and 15b compare Levec prewetted with Kan prewetted beds at the same flow conditions.

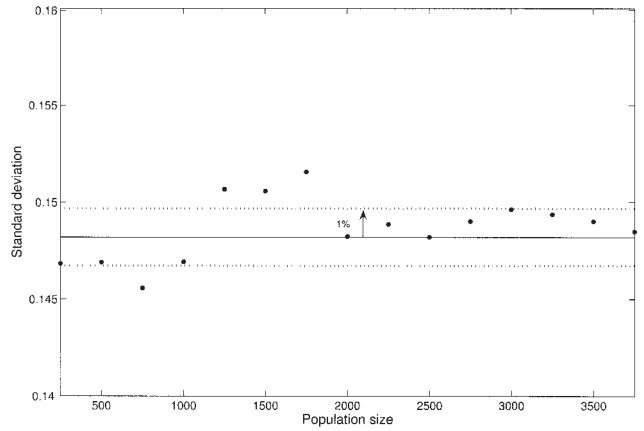

Figure 9. Standard deviation as a function of population size.

The standard deviation stabilizes within a population size of 2000 particles.

Table 2. Liquid Holdup and Pressure Drop Measurements

L (kg m^{-2} s^{-1})	G (kg m^{-2} s^{-1})	Prewetting Procedure	Liquid Holdup	Pressure Drop (Pa m^{-1})
1.60	0.023	Kan	0.15	139
1.60	0.152	Kan	0.15	2020
1.60	0.152	Levec	0.07	910
5.35	0.023	Kan	0.24	540
5.35	0.152	Kan	0.22	4510
5.35	0.152	Levec	0.14	1879

Discussion

Kan prewetted beds

For all Kan prewetted beds, all of the packing was in some fashion contacted by the flowing liquid, regardless to the liquid or gas flow rates. One can expect that this will also be the case for Kan prewetted beds at any flow conditions, and that the entire catalyst will at least be used to some extent in Kan prewetted beds. The shapes of all distributions are very similar, hinting that the same type of flow was present in all beds and that the flow type was independent of the liquid and gas flow rates. Literature results state that Kan prewetted beds exclusively exhibit film flow.[6,7,9] The PWDs of the beds that were exposed to the high liquid rate do, however, have higher peaks than those for the lower liquid flow rate, which shows that increasing liquid flow rate causes the liquid to be more homogeneously distributed.

Very little effect of the gas flow rate is evident from Figure 13. For both liquid flow rates that were investigated, the average wetting efficiency is higher for a higher gas flow rate, but only marginally. The correlation proposed by Al-Dahhan and Dudukovic[17] also predicts only a slight influence of the gas flow rate at the experimental flow conditions, whereas the other correlations shown in Figure 10 do not predict any influence of the gas flow rate.

Levec prewetted beds

It is clear that the PWDs for Levec prewetted beds differ significantly from those for Kan prewetted beds. A significant fraction of particles is very poorly wetted or even completely dry, so that parts of a Levec prewetted bed may not be used whatsoever. This effect is more significant at the lower liquid flow rate. Apart from the differences in PWDs, average wetting efficiencies are far lower for the Levec prewetted beds than for the Kan prewetted beds at corresponding liquid and gas flow rates (see Figure 13).

That the distribution of liquid in Levec prewetted beds is completely different from that in Kan prewetted beds becomes evident when one compares Levec- and Kan prewetted beds that have the same wetting efficiency (Levec: L= 5.35 kg m^{-2} s^{-1}, G = 0.152 kg m^{-2} s^{-1}; Kan: L = 1.60 kg m^{-2} s^{-1}, G = 0.023 kg m^{-2} s^{-1}). Even for the same average wetting efficiencies, PWDs of the two prewetting modes look completely different, and it is evident that the liquid flow morphologies of the two prewetting modes differ dramatically. Literature suggests that filament and film flows are present in Levec prewetted beds.[6] The description of two flow types is supported by the fact that the PWDs for the Levec prewetted beds appear to be bimodal, that is, they exhibit two local maxima. If this description of flow morphology in Levec prewetted beds can be adopted, it implies that filament flow is the source of the significant amount of particles that are poorly wetted. As the liquid flow rate is increased, the PWD becomes more similar in shape to the PWDs obtained for the Kan prewetted beds. In terms of the film/filament flow description of the trickle-flow morphology, this means that increased liquid flow rate favors the formation of films, and the fraction of filament flow is decreased by an increased liquid flow rate. This is in accordance with the findings of Christensen et al.[6]

Possible implications in reactor modeling and performance

Most trickle-bed reactor modeling was previously performed by using only the (overall) average wetting efficiency of a bed. Having wetting distributions available, one can now evaluate whether such an approach is accurate enough or whether the distribution of particle wetting should be taken into account.

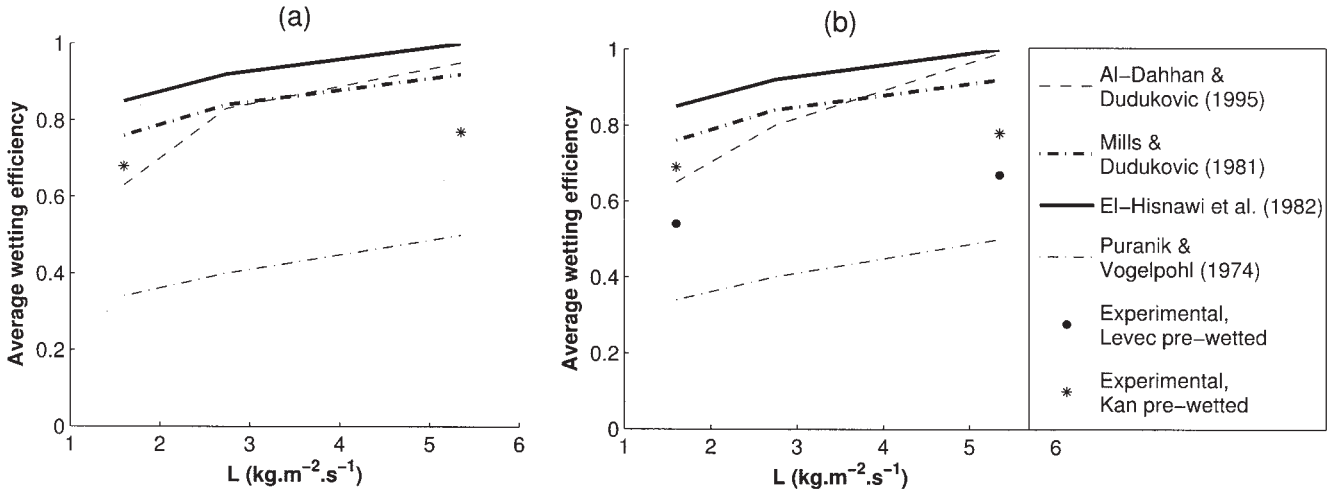

Figure 10. Comparison of experimental average wetting efficiencies with existing correlations.

(a) G = 0.023 kg m^{-2} s^{-1} and (b) G = 0.152 kg m^{-2} s^{-1}.

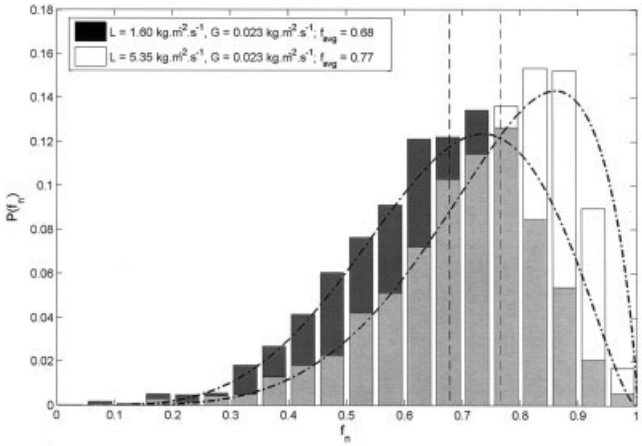

Figure 11. Particle wetting distributions for Kan prewetted beds with *L* values of 1.60 and 5.35 kg m^{-2} s^{-1}.

Gas flow rate was $G = 0.023$ kg m^{-2} s^{-1}.

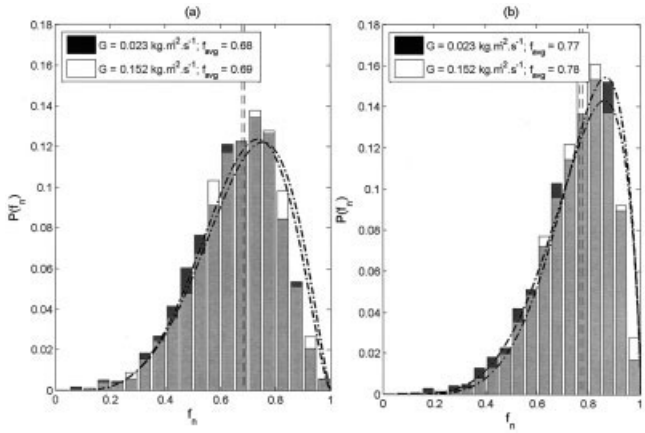

Figure 13. Wetting distributions for Kan prewetted beds with *G* values of 0.023 and 0.152 kg m^{-2} s^{-1} with (a) $L = 1.60$ kg m^{-2} s^{-1} and (b) $L = 5.35$ kg m^{-2} s^{-1}.

Liquid-limited reactions

Based on the model of Dudukovic,[1] liquid-limited trickle-bed reactor efficiencies was calculated by using three different approaches:

(1) Make use of the overall average wetting efficiency. The average wetting trickle-bed efficiency is then given by[1]

$$\eta_{TB} = f_{avg} \frac{\tanh\left(\frac{\phi}{f_{avg}}\right)}{\phi} \tag{3}$$

Note that in this model, only the effect of fractional wetting on internal mass transfer limitations is accounted for.

(2) Calculate the trickle-bed efficiency for each particle, and then take the average of all the obtained trickle-bed efficiencies. The wetting distribution trickle-bed efficiency is then given by

$$\eta_{TB} = \sum^{n} \left(P(f_n) f_n \frac{\tanh\left(\frac{\phi}{f_n}\right)}{\phi} \right) \tag{4}$$

(3) Beaudry et al.[4] proposed a PWD in trickle-bed reactors consisting of only completely wetted half-wetted and completely dry particles (Eq. 2). Trickle-bed efficiencies that were calculated with Eq. 4 and the PWD proposed by Beaudry et al.[4] are referred to as Beaudry distribution trickle-bed efficiencies.

Average wetting, wetting distribution,and Beaudry distribution trickle-bed efficiencies are compared in Figures 16 and 17 for the different PWDs and different values of the Thiele modulus. For all Kan prewetted beds that were investigated, the liquid-limited trickle-bed efficiency can well be estimated with

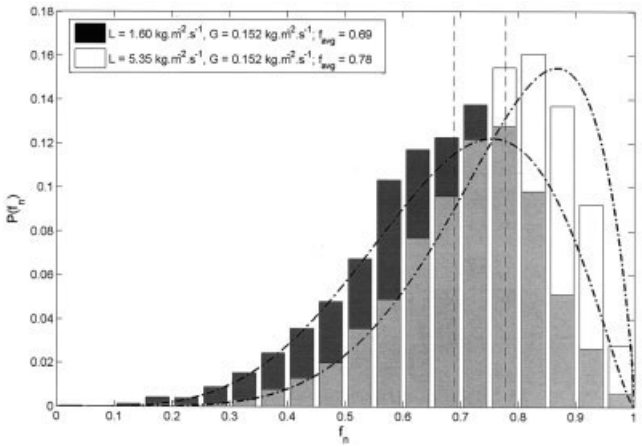

Figure 12. Particle wetting distributions for Kan prewetted beds with *L* values of 1.60 and 5.35 kg m^{-2} s^{-1}.

Gas flow rate was $G = 0.152$ kg m^{-2} s^{-1}.

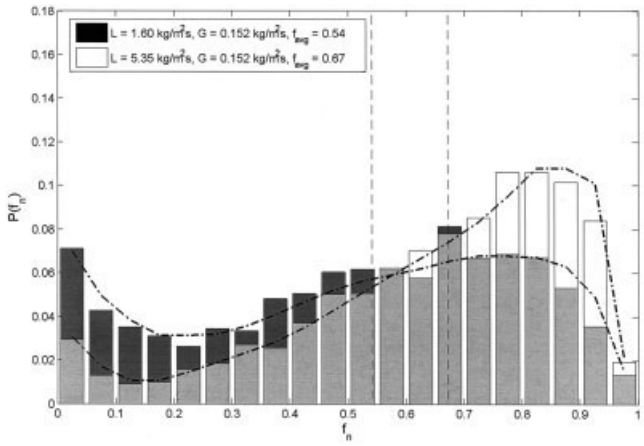

Figure 14. Particle wetting distributions for Levec prewetted beds with *L* values of 1.60 and 5.35 kg m^{-2} s^{-1}.

Gas flow rate was $G = 0.152$ kg m^{-2} s^{-1}.

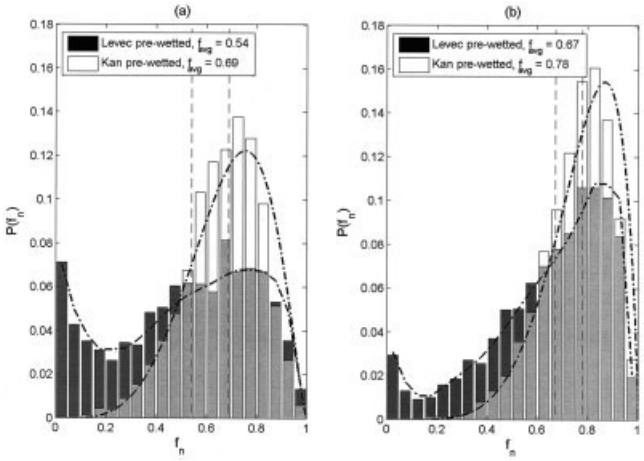

Figure 15. Particle wetting distributions for Levec- and Kan prewetted beds at the same gas and liquid flow rates.

(a) $L = 1.60$ kg m^{-2} s^{-1} and $G = 0.152$ kg m^{-2} s^{-1}; (b) $L = 5.35$ kg m^{-2} s^{-1} and $G = 0.152$ kg m^{-2} s^{-1}.

one average value for the wetting efficiency. All particles were well wetted, so that the PWD proposed by Beaudry et al.[4] underestimates liquid-limited trickle-bed efficiency as a function of average wetting in Kan prewetted beds at low values of the Thiele modulus.

Using only an average wetting efficiency can lead to errors when modeling a Levec prewetted bed, especially at low liquid flow rates. The reason for this is that a large fraction of particles is very poorly wetted or even completely dry. The PWD proposed by Beaudry et al.,[4] however, overestimates the fraction of very poorly wetted (completely dry) particles. For $\phi > 2$, only the average wetting, and not its distribution, determines the liquid-limited trickle-bed efficiency, given that the relationship between the fractional wetting of a particle and its efficiency becomes linear (Eq. 4).

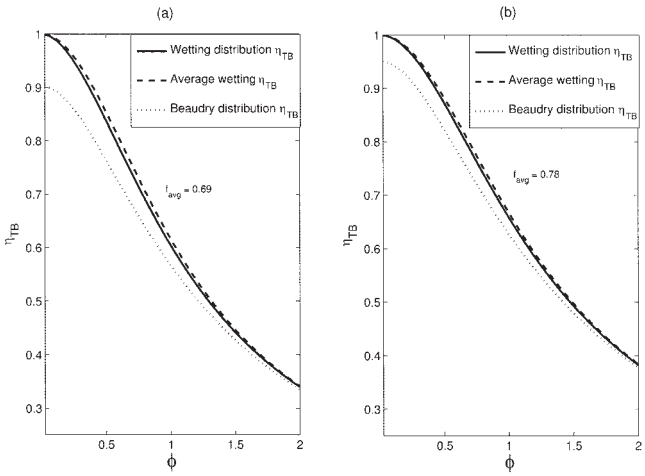

Figure 16. Average wetting, wetting distribution, and Beaudry distribution liquid-limited trickle-bed efficiencies as functions of Thiele modulus in Kan prewetted beds.

(a) $L = 1.60$ kg m^{-2} s^{-1} and (b) $L = 5.35$ kg m^{-2} s^{-1}. The gas flow rate was $G = 0.152$ kg m^{-2} s^{-1}.

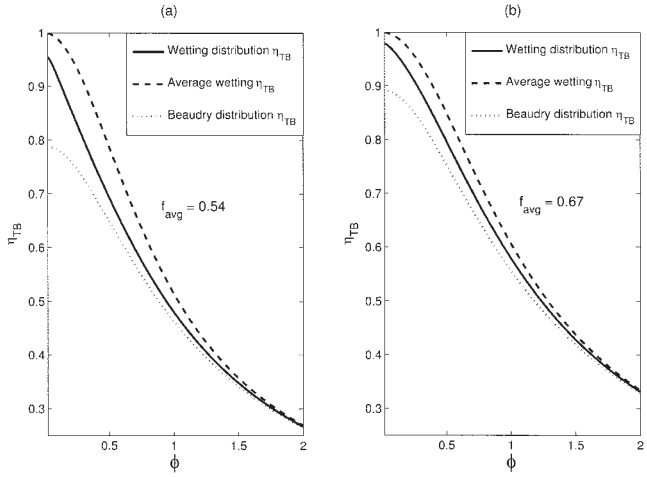

Figure 17. Average wetting, wetting distribution, and Beaudry distribution liquid limited trickle-bed efficiencies as functions of Thiele modulus in Levec prewetted beds.

(a) $L = 1.60$ kg m^{-2} s^{-1} and (b) $L = 5.35$ kg m^{-2} s^{-1}.

Trickle-bed efficiencies as functions of particle Thiele modulus for Levec- and Kan prewetted beds at the same flow conditions are compared in Figure 18. As expected, Levec prewetted beds are considerably inferior to Kan prewetted beds at the same flow condition for liquid-limited reactions.

Gas-limited reactions

The effect of wetting efficiency on gas-limited reactions is most evident when external liquid–solid mass transfer limitations are significant. When this is the case, most trickle-bed reactor models predict an increase in trickle-bed efficiency as the average wetting efficiency is decreased.[3,22,23] The reason for this is that gas–solid mass transfer is much faster than gas–liquid–solid mass transfer, so that the surface concentration of the limiting reagent will be much higher at dry catalyst surfaces

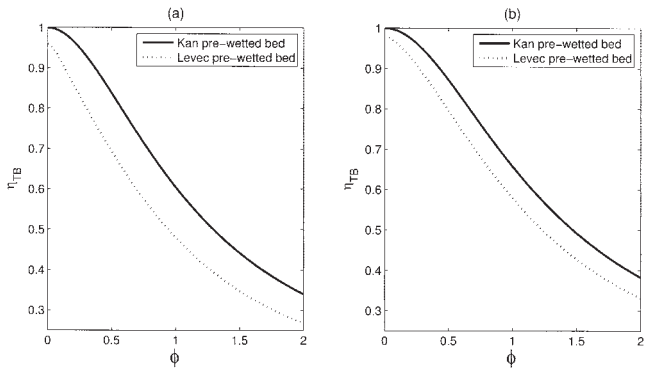

Figure 18. Comparison of liquid-limited trickle-bed efficiencies for the different prewetting modes.

(a) $L = 1.60$ kg m^{-2} s^{-1} and (b) $L = 5.35$ kg m^{-2} s^{-1}. Gas flow rate was $G = 0.152$ kg m^{-2} s^{-1}.

than at wetted surfaces. There is, however, evidence of internal depletion of the liquid side reagent when particles are very poorly wetted and internal diffusion limitations of the liquid-side reagent are significant.[4,24] This depletion has a detrimental effect on reactor performance.

Based on average wetting efficiencies, Levec prewetted beds will be superior to Kan prewetted beds under gas-limited conditions. Based on the PWDs presented herein, however, one should consider that Levec prewetted beds are far more likely to exhibit liquid limitations than Kan prewetted beds because of the large amount of poorly wetted particles in which depletion of the liquid side reagent can take place. When no significant external liquid–solid mass transfer limitations are present, Kan prewetted beds will be superior to Levec prewetted beds, given that the latter contain completely dry particles that are always detrimental to reactor performance. Both effects described above will become increasingly significant as the liquid flow rate is decreased.

Conclusions

A new technique, based on the colorimetric method of Lazzaroni et al.,[15] was developed for the express purpose of investigating the distribution of particle wetting in trickle-bed reactors.

It was shown that the manner in which a trickle-bed is prewetted before flow can greatly influence its wetting efficiency. Average wetting efficiencies of the Kan prewetted beds were significantly higher than those for the Levec prewetted beds at corresponding liquid and gas flow rates. Considerable differences in the PWDs for the two prewetting modes show that trickle-flow patterns can be manipulated by the manner in which a bed is prewetted.

In all Kan prewetted beds, all of the particles were in some fashion contacted by the flowing liquid. The shapes of the PWDs were consistent, thus suggesting that flow in Kan prewetted beds was stable and very similar for all experimental flow conditions. Increasing liquid flow rate causes flow in Kan prewetted beds to be distributed more homogeneously.

The Levec prewetted beds contained a large amount of dry and poorly wetted particles, especially at the lower liquid flow rate. The shapes of the distributions are very different from those of Kan prewetted beds, and two local maxima suggest two different types of flow—film and filament flow—according to the literature.[6] If this explanation is adopted, increasing liquid flow rate favors the formation of films, and flow in a Levec prewetted bed will tend to approach that in a Kan prewetted bed as the liquid flow rate is increased.

The effect of the obtained PWDs on reactor modeling and performance showed that one might need to take into account not only average wetting efficiency, but also particle wetting distributions when modeling a Levec prewetted bed for both liquid- and gas-limited reactions, arising from the large amount of poorly wetted and completely dry particles. The PWD proposed by Beaudry et al.,[4] however, overestimates the amount of completely dry particles in a trickle-bed reactor. For liquid-limited reactions, Kan prewetted beds can be modeled satisfactorily with the average wetting efficiency only. The effect of prewetting on reactor performance is quite evident: Kan prewetting will give superior results for liquid-limited reactions. When modeling gas-limited reactions, Levec prewetting will outperform Kan prewetted beds when only considering the average wetting efficiency. The opposite results may be found when PWDs are taken into consideration, resulting from liquid limitations on poorly wetted particles.

Notation

D_{eff} = effective diffusivity, $m^2\ s^{-1}$
d_p = particle diameter, m
F = fractional wetting of a particle
F_A = mole flow rate of reagent A, mol/s
$f$avg = average wetting efficiency
f_n = fractional wetting bin
G = gas mass flux, kg $m^{-2}\ s^{-1}$
k = first-order reaction rate constant, s^{-1}
L = liquid mass flux, kg $m^{-2}\ s^{-1}$
$P(f)$ = fraction of catalyst with fractional wetting f
$P(f_n)$ = fraction of catalyst with fractional wetting f, where $f_n-0.025 < f < f_n+0.025$
R = particle radius on image, pixels
r = maximum distance away from center pixel for which a pixel is still taken into account, pixels
r_A = rate of consumption of reagent A, mol (kg catalyst)$^{-1}$ s^{-1}
W = mass of catalyst, kg
η_{TB} = trickle-bed efficiency compared to that of an ideal plug flow reactor
ϕ = first-order reaction particle Thiele modulus, $\phi = (6/d_p)\sqrt{k/D_{eff}}$

Literature Cited

1. Dudukovic MP. Catalyst effectiveness factor and contacting efficiency in trickle-bed reactors. *AIChE J.*1977;23:940-4.
2. Mills PL, Dudukovic MP. Analysis of catalyst effectiveness in trickle-bed reactors processing volatile or non-volatile reactants. *Chem Eng Sci.* 1980;35:2267-2279.
3. Herskowitz M, Carbonell RG, Smith JM. Effectiveness factors and mass transfer in trickle-bed reactors. *AIChE J.* 1979;25:272-283.
4. Beaudry EG, Dudukovic MP, Mills PL. Trickle-bed reactors: Liquid diffusional effects in a gas-limited reaction. *AIChE J.*1987;33:1435-47.
5. Kan KM, Greenfield PF. Multiple hydrodynamics in concurrent two-phase downflow through packed beds. *Ind Eng Chem Process Des Dev.* 1978;17:482-485.
6. Christensen G, McGovern SG, Sudaresan G. Concurrent downflow of air and water in a two-dimensional packed column. *AIChE J.* 1986; 32:1677.
7. Lutran PG, Ng KM, Delikat EP. Liquid distribution in trickle-beds. An experimental study using computer-assisted tomography. *Ind Eng Chem Res.* 1991;30:1270-1280.
8. Ravindra PV, Rao DP, Rao MS. Liquid flow texture in trickle-bed reactors: An experimental study. *Ind Eng Chem Res.* 1997;36:5133-5145.
9. Sederman AJ, Gladden LF. Magnetic resonance imaging as a quantitative probe of gas–liquid distribution and wetting efficiency in trickle-bed reactors. *Chem Eng Sci.* 2001;56:2615-2628.
10. Van der Merwe W, Nicol W. Characterization of multiple flow morphologies within the trickle flow regime. *Ind Eng Chem Res.* 2005;44: 9446-9450.
11. Levec J, Grosser K, Carbonell RG. The hysteretic behavior of pressure drop and liquid holdup in trickle beds. *AIChE J.* 1988;34:1027-1030.
12. Wang R, Mao Z, Chen J. Experimental and theoretical studies of pressure drop hysteresis in trickle bed reactors. *Chem Eng Sci.*1995; 50:2321-28.
13. Zimmerman SP, Ng KM. Liquid distribution in trickling flow trickle-bed reactors. *Chem Eng Sci.* 1986;41:861-866.
14. Burghardt A, Bartelmus G; Jaroszynski M, Kolodziej A. Hydrodynamics and mass transfer in a three-phase fixed-bed reactor with concurrent gas–liquid downflow. *Chem Eng J.*1995;58:83-.

15. Lazzaroni CL, Kesselman HR, Figoli HS. Colorimetric evaluation of the efficiency of solid–liquid contacting in trickle-bed reactors. *Ind Eng Chem Res.* 1988;27:1132-1135.
16. Van der Merwe W, de Beer FC, Nicol W. Internal catalyst wetting dynamics of porous α- and γ-alumina spheres by X-ray tomography. *South African J Sci.* 2006;00:000-0.
17. Al-Dahhan MH, Dudukovic MP. Catalyst wetting efficiency in trickle-bed reactors at high pressure. *Chem Eng Sci.*1995;50:2377-89.
18. Mills PL, Dudukovic MP. Evaluation of liquid–solid contacting in trickle-bed reactors by tracer methods. *AIChE J.* 1981;27:893-903.
19. El-Hisnawi AA, Dudukovic MP, Mills PL. Trickle-bed reactors: Dynamic tracer tests, reaction studies and modelling of reactor performance. *ACS Symp Ser.* 1982;196:421.
20. Lakota A, Levec J. Solid–liquid mass transfer in packed beds with cocurrent downward two-phase flow. *AIChE J.* 1990;36:1444-1448.
21. Puranik SS, Vogelpohl A. Effective interfacial area in irrigated packed columns. *Chem Eng Sci.* 1974;29:501-507.
22. Ramachandran PA, Smith JM. Effectiveness factors in trickle-bed reactors. *AIChE J.* 1979;25:538-542.
23. Tan CS, Smith JM. Catalyst particle effectiveness with unsymmetrical boundary conditions. *Chem Eng Sci.* 1980;35:1601-1609.
24. Ruiz P, Crine M, Germain A, L'Homme G. Influence of the reactional system on the irrigation rate in trickle-bed reactors. *ACS Symp Ser.* 1984;237:15.

Manuscript received Apr. 3, 2006, and revision received Jun. 23, 2006.